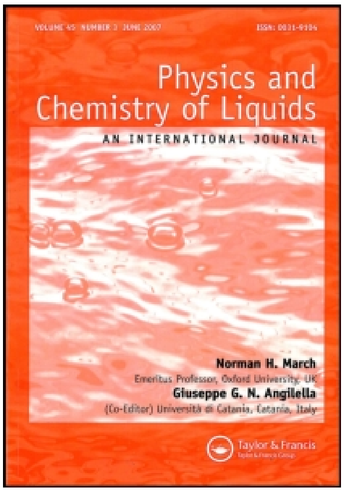

Physics and Chemistry of Liquids
Publication details, including instructions for authors and subscription information:
http://www.informaworld.com/smpp/title~content=t713646857

The Calculation of Liquid-Vapor Equilibrium for Group Ia and Group Iia Metals

Mark Montoya[a]; T. J. Anderson[b]; K. Runge[c]
[a] Department of Chemical Engineering, New Mexico State University, Las Cruces, NM [b] Department of Chemical Engineering, University of Florida, Gainesville [c] Department of Physics, University of Florida, Gainesville

To cite this Article Montoya, Mark , Anderson, T. J. and Runge, K.(1995) 'The Calculation of Liquid-Vapor Equilibrium for Group Ia and Group Iia Metals', Physics and Chemistry of Liquids, 29: 3, 169 — 181
To link to this Article: DOI: 10.1080/00319109508028423
URL: http://dx.doi.org/10.1080/00319109508028423

Phys. Chem. Liq., 1995, Vol. 29, pp. 169–181
Reprints available directly from the publisher
Photocopying permitted by license only

THE CALCULATION OF LIQUID-VAPOR EQUILIBRIUM FOR GROUP IA AND GROUP IIA METALS

MARK MONTOYA

Department of Chemical Engineering, New Mexico State University, Box 30001/Dept. 3805 Las Cruces, NM 88003

T. J. ANDERSON

Department of Chemical Engineering, University of Florida, Gainesville, FL32611

and

K. RUNGE

Department of Physics, University of Florida, Gainesville, FL32611

(Received 11 October 1994)

Liquid-vapor coexistence curves for selected group IA and IIA metals are calculated. The Gibbs-Bogoljubov variational method is used to find a least upper bound to the Helmholtz energy of the liquid phase. The hard sphere liquid is chosen to represent the structure of the metal melt, and the empty-core pseudopotential is chosen to the model the potential energy of interaction in the liquid phase. The vapor phase is modeled as an ideal gas mixture of monomers and dimers, with the distribution of mole fractions determined by the canonical ensemble partition function. Parameters are chosen that model coexistence properties between the melting temperature and the boiling temperature of the liquid metals. Good results are obtained for representative group IA and group IIA metals.

KEY WORDS: Pseudopotential, dimers, liquid-vapor coexistence, thermodynamic properties, Group IA, Group IIA, hard spheres.

INTRODUCTION

From a materials processing standpoint, an estimation of the thermodynamic properties of liquid metal systems is important when defining process limitations. Processing methods such as melt-zone refinement, rapid thermal processing, and bulk crystal growth require knowledge of liquid vapor coexistence for process design. Similarly, the mechanics of laser ablation techniques for thin film deposition are limited by the thermodynamics of the metals involved in the system. The experimental measurement of thermodynamic properties for saturated metal systems is difficult; not only are the temperatures involved very high, but the metal is often very reactive at high temperatures. Thus, it is important that methods are developed that allow for the theoretical prediction of metal coexistence properties.

As the complexity of metal alloys increase, so do the permutations available for alloy design. The development of an accurate, predictive theory for the thermodynamic properties of liquid metal melts becomes important to minimize the multitude of experiments that will be necessary to characterize liquid-vapor coexistence behavior. Before simple models are applied to more complex binary systems, parameters and models must be developed and refined for single component systems. This paper addresses such refinement.

A recent attempt at modeling sodium liquid-vapor coexistence properties has given satisfactory results from the melting temperature to near the critical temperature[1]. Improvements from older techniques[2] include the modeling of dimers in the metal liquid phase, and parameterization of the first Fourier component of the empty-core pseudopotential to match the experimental internal energy of the liquid system at its melting temperature. In this paper, this approach has been extended to the group IA and group IIA metals for which experimental spectroscopic data is available for dimer species.

LIQUID THEORY

The theory for the calculation for the Helmholtz energy of the liquid phase is established[3], but an outline of the theory is provided to establish the differences between these calculations and the results from previous attempts. The Helmholtz energy of the liquid system is

$$F = F_{\mathrm{hs}} + \mathrm{F}_{\mathrm{ps}} \tag{1}$$

where F_{hs} is the contribution to the Helmholtz energy from the entropy of an ideal liquid and the entropy of the reference fluid, and F_{ps} is the contribution to energy due to the arrangement of core ions within the electron gas. The contributions due to the interactions of ion cores with the electron gas are model dependent, and for the empty-core pseudopotential model these contributions are

$$F_{\mathrm{ps}} = \mathrm{F}_{\mathrm{eg}} + \mathrm{F}_1 + \mathrm{F}_2 + \mathrm{F}_M \tag{2}$$

where F_{eg} is the contribution due to the electron gas medium, F_1 is the zeroth Fourier component contribution, F_2 is the second order (or band structure) energy, and F_M is the Madelung contribution to the energy of the system.

The four contributions to the Helmholtz energy of the liquid system are given by

$$F_{\mathrm{eg}} = z\left(\frac{3}{10}k_F^2 - \frac{3}{4\pi}k_F - 0.0474 - 0.0155\ln(k_F) - \frac{1}{2}\gamma_{\mathrm{eg}}T^2\right) \tag{3}$$

$$F_1 = nZ\left[\lim_{q\to 0}\left(v(q) + \frac{4\pi Z}{q^2}\right)\right] \tag{4}$$

$$F_2 = \frac{1}{16\pi^3}\int_0^\infty a(q,n)\,v(q)^2\left(\frac{1}{\varepsilon(q,n)} - 1\right)q^4\,dq \tag{5}$$

$$F_M = \frac{1}{\pi}\int_0^\infty Z^2(a(q,n)-1)\,dq \tag{6}$$

where K_F is the magnitude of the Fermi wavevector, n is the ion core density of the fluid, $\varepsilon(q,n)$ is the dielectric function of an electron gas, Z is the metal valence, $v(q)$ is the electron-ion pseudopotential, $a(q,n)$ is the structure factor of the reference fluid, and γ_{eg} is the constant volume heat capacity of the electron gas. The electron gas energy includes the terms for electron-electron repulsion, and the exchange and correlation energy contributions due to Nozieres and Pines[4]. The rigorous expression for the low temperature value of the electron heat capacity normally has exchange and correlation terms[5], but the independent Fermion result

$$\gamma_{eg} = \left(\frac{\pi k_B}{k_F}\right)^2 \tag{7}$$

is expected to give accurate results throughout the temperature range of these simulations. The Itsimaru-Utsumi approximation to the electron gas dielectric function $\varepsilon(q,n)$ is chosen for its simplicity and accuracy[6].

A system of hard spheres is chosen as the reference fluid for this calculation; this choice of reference system simplifies some of the terms present in the expression for the pseudopotential contribution to Helmholtz energy. An analytic approximation to the hard sphere structure factor is found by solving the Percus-Yevick equation, avoiding the need for molecular dynamics simulation at each density[7]. The expression for the Madelung contribution to the Helmholtz energy is also simplified to the analytic expression $F_M = Z^2\alpha_M$ where

$$\alpha_M = \frac{2\pi n Z^2}{1+2\eta}\left[-\sigma^2 - \frac{1}{5}\left(1-\frac{\eta}{2}\right)\sigma^2\right] \tag{8}$$

and η is the packing fraction for a hard sphere fluid, given in terms of the density n and the hard sphere diameter σ by

$$\eta = \frac{\pi\sigma^3 n}{6}. \tag{9}$$

The electron-ion pseudopotential chosen for this application is the empty-core potential model[8]

$$v(q) = -\frac{4\pi}{q^2}Z\cos(qR_c) \tag{10}$$

Substitution of (10) into (4) leads to the result

$$F_1 = 2\pi n Z^2 R_c^2 \tag{11}$$

which though analytically correct often leads to a poor representation of the Helmholtz energy of the liquid metal system. Other atempts at calculating the liquid-vapor coexistence curves for sodium metal have corrected F_1 by introducing a cubic polynomial expression in terms of density for the energy contribution[1], which has coefficients fit to reproduce experimental density measurements of the saturated liquid phase. Since the emphasis of this study is the creation of a predictive tool to be used for calculation of engineering properties, the experimental parameters gathered are kept to a minimum, and the cubic polynomial representation of the first Fourier component is eliminated.

Terms that contribute to the Helmholtz energy due to the choice of the hard sphere reference system are also well defined. The Helmholtz energy of the hard sphere system F_{hs} has two terms

$$F_{\text{hs}} = \frac{3}{2} k_B T - T S_{\text{hs}} \tag{12}$$

The hard sphere entropy

$$S_{\text{hs}} = S_{\text{gas}} + S_{\eta} \tag{13}$$

is composed of the ideal term

$$S_{\text{gas}} = \ln\left[\frac{e}{n}\left(\frac{emk_B T}{2\pi h^2}\right)^{3/2}\right] \tag{14}$$

where m is the mass of an atom, and the contribution due to the entropy of the ideal hard sphere fluid

$$S_{\eta} = \ln(1-\eta) + \frac{3}{2}\left[1 - \frac{1}{(1-\eta)^2}\right] \tag{15}$$

The hard-sphere model has the single variational parameter σ. Thus, the least upper bound to the Helmholtz energy is calculated by minimizing the right-hand side of equation (1) with respect to the hard sphere diameter. A single variational condition defines this minimum

$$\left(\frac{\partial F}{\partial \sigma}\right)_{\Omega,T} = 0 \tag{16}$$

This condition also simplifies the expressions for the entropy and the pressure of the system writen in terms of the total Helmholtz energy of the system, which are now given by the partial derivatives

$$S = -\left(\frac{\partial F}{\partial T}\right)_{\Omega,\sigma} \tag{17}$$

and

$$P = n^2\left(\frac{\partial F}{\partial n}\right)_{T,\sigma} = -\left(\frac{\partial F}{\partial \Omega}\right)_{T,\sigma} \tag{18}$$

Once the Helmholtz energy is known, the Gibbs energy, which is the chemical potential of a single-component system, is found by making a pressure-volume correction to the approximated Helmholtz energy

$$\mu = G = F + PV \tag{19}$$

The Gibbs energy of a system is calculated from the canonical ensemble partition function of a system[9,10], so that if the relevant energy levels of system are known, the population of states is also known, and the Gibbs energy for that system can be calculated. If an ideal gas model is chosen for the monomers of the system, and a rigid rotor approximation for the dimers, constants found using vapor phase spectroscopy will yield the information necessary to calculate the Gibbs energy of an ideal gas consisting of monomers and dimers.

Assume a vapor system with a constant number of atoms N, which is made up of N_1 monomers and N_2 dimers. The number of atoms in the vapor phase is fixed, so that

$$N = N_1 + 2N_2 \tag{20}$$

Both constituent 1 and constituent 2 are assumed to occupy the volume of the system V. The Helmholtz energy of this system consists of two contributions

$$F = F_1 + F_2 \tag{21}$$

Both terms are expressed in terms of the canonical ensemble partition function Z_i, which for each species i in the gas phase contributes

$$F_i = -\frac{N_i k_B T}{N} \ln\left(\frac{eZ_i}{N_i}\right) \tag{22}$$

to the Helmholtz energy.

The partition function each the monomer is given by the expression

$$Z_1 = g\left(\frac{M k_B T}{2\pi \hbar^2}\right)^{3/2} V \equiv \zeta_1 V \tag{23}$$

where g is the degeneracy due to spin and angular momentum of the system. This partition function assumes the monomer is a non-interacting collection of point masses of mass M.

The dimer is modeled as a rigid rotor, which allows the approximation of the rotational and vibrational contributions to the Helmholtz energy. The partition function for the rigid rotor is

$$Z_2 = \left(\frac{2\pi M k_B T}{2\pi \hbar^2}\right)^{3/2} V \exp\left(\frac{\varepsilon_b}{k_B T}\right)\left(\frac{T k_B M R^2}{2\hbar^2}\right)\left(\frac{k_B T}{\hbar\omega}\right) \equiv \zeta_2 V \tag{24}$$

given the diatomic binding energy ε_b, the bond length between atoms in the diamotic R, and the angular frequency of vibration ω. The last two factors in (24) correspond to contributions to the partition function due to rotational and vibrational modes, respectively. It is assumed that the high temperature approximation to this partition function is valid, and experimental values for metals in their vapor state confirm the validity of this assumption.

The pressure of the system is calculated from the volume derivative of the Helmholtz energy

$$P=-\left(\frac{\partial F}{\partial V}\right)_T=\sum_i P_i=\sum_i \frac{N_i k_B T}{V} \tag{25}$$

The Gibbs energy per atom is given by

$$G=F+PV=-\sum_i \frac{N_i k_B T}{N}\ln\left(\frac{Z_i}{N_i}\right) \tag{26}$$

from which the chemical potential for each constituent is calculated and equated to satisfy the conditions of thermodynamic equilibrium. If this is done for the dimerization reaction

$$2X \leftrightarrow X_2$$

then chemical equilibrium must satisfy

$$2\left(\frac{\partial G}{\partial N_1}\right)=\left(\frac{\partial G}{\partial N_2}\right)=\lambda^{1/2} \tag{27}$$

where λ is a constant corresponding to the square root of the chemical potential of the diatomic. Two expressions result from this equilibrium equation: $N_1=\lambda Z_1$ and $N_2=\lambda^2 Z_2$. The fraction of each atom in the gas phase is expressed as a function of λ and the specific volume of the vapor Ω_v

$$\frac{N_1}{N}=\lambda\zeta_1\Omega_v \tag{28}$$

$$\frac{N_2}{N}=\lambda^2\zeta_2\Omega_v \tag{29}$$

which satisfies the requirement that the sum of the fractions of each constituent must be one

$$(\lambda\zeta_1+2\lambda^2\zeta_2)\Omega_v=1 \tag{30}$$

The system pressure is now defined in terms of the partition function result

$$P_v=(\lambda\zeta_1+\lambda^2\zeta_2)k_B T, \tag{31}$$

and the Gibbs energy of the system is the simple expression

$$G_v=k_B T\ln\lambda \tag{32}$$

The contributions to the Gibbs energy due to the electron occupation of excited states is assumed to be very small, since the electronic energies involved contribute little to the Helmholtz energy at the temperatures of interest. For metals with high critical points, it is increasingly important to include electronic terms in the canonical ensemble to increase the accuracy of the energy in the vapor phase calculation.

COMPUTATIONAL PROCEDURE

A computational procedure for the calculation of saturated conditions is now outlined. If the Gibbs energy of the liquid phase is equated with the Gibbs energy of the vapor phase, an expression for λ at equilibrium is apparent, and given by

$$\lambda(\Omega_l) = \exp\left(\frac{F_l(\Omega_l) - \Omega_l \left(\frac{\partial F(\Omega_l)}{\partial \Omega_l} \right)_{T,\sigma} - E_{\text{ion}}}{k_B T} \right) \tag{33}$$

where E_{ion} is used to correct the liquid energy to the same reference as the monatomic vapor[2]. The pressure equation allows for construction of an equation that defines equilibrium for the system

$$-\left(\frac{\partial F_l(\Omega_l)}{\partial \Omega_l} \right)_{T,\sigma} = (\lambda(\Omega_l)\zeta_l + \lambda(\Omega_l)^2 \zeta_2) k_B T \tag{34}$$

Since equation (34) is a function of liquid volume only, solutions are found by bracketing the roots and using a numerical root finder to solve for liquid volume. Once the liquid volume is found, information on the pressure, monatomic and diatomic fractions, Gibbs energy, and vapor volume immediately follows.

PARAMETERS

The calculation of vapor liquid equilibrium is influenced by small changes in the calculated Gibbs energy of the liquid and vapor systems. Small errors in the Gibbs energy calculation may result in large deviations from experimental data. Several parameters are available in the calculation that allow adjustments that compensate for the deviation of the experimental Helmholtz energy of the liquid system from the Helmholtz energy calculated using the empty-core pseudopotential.

As is the philosophy of other calculations, the first Fourier component of the Helmholtz energy is adjusted so that the calculated internal energy of the liquid system at the melting temperature matches an experimental value. The calculated internal energy of the liquid system is given by the five terms

$$U_{\text{liq}} = \frac{3}{2} k_B T + F_M + F_1 + F_2 + F_{\text{eg}}$$

In order to calculate the coefficient for the adjusted first Fourier component, the temperature and density of the liquid are fixed to the experimental value, and the internal energy of the liquid calculated. The first Fourier component, F_1, is adjusted until the calculated internal energy matches the experimental internal energy of the system.

A second adjustment to the calculation involves the relative zeroes of energy between the liquid and the vapor phase. The quantity E_{ion}, which represents the energy needed to excite the valence electrons from the outer electron shell into the conduction band of the liquid metal, is calculated so that the equilibrium condition given by (34) is satisfied at the boiling point of the metal.

The parameters incorporated into the liquid-vapor coexistence model are given in Table 1. Third decimal place corrections are made to the experimental internal energy for each of the metal systems. The degeneracy g for the rigid rotor dimer model is one of the group IA elements, and two for the group IIA elements.

RESULTS

The liquid density versus temperature plot for group IA metals is shown in Figure 1, and the group IIA metals studied are shown in Figure 2. The calculated results agree closely with assessed thermodynamic data between the melting temperature and boiling temperature of the metal systems. Above the melting temperature, there is a trend in calculation away from the assessed data. The calculated liquid density is higher than the assessed experimental data at the same temperature, and this deviation increases with increasing temperature.

The calculated vapor pressures of the saturated metal systems are in good agreement with assessed experimental data. Figure 3 compares the plots of $\log_{10}$(pressure) versus inverse temperature for the Group IA systems. The calculated data is nearly linear, indicating a constant heat of vaporization for each of the metals over the entire temperature range of the system. The same is true for the Group IIA metals illustrated in Figure 4.

The results from Osman and Young[1] show calculated monomer fractions that deviate from experimental data at high temperature. Each of the metals calculated in this survey show the same deviation. Monomer fractions are too high at lower temperatures, but as the temperature increases above the boiling temperature, the monomer fraction becomes smaller than that experimentally observed. Decreased monomer fraction at a given temperature decreases the calculated pressure and Gibbs energy of the vapor system below experimental values. Since the Gibbs energy of the liquid system increases with decreasing density along the saturated properties curve for the metal systems, the liquid density is affected, leading to the calculation of liquid densities that are too high at temperatures above the boiling temperature.

Table 2 shows the calculated values for the ionization energy of the metal system, and compares the values to those obtained through experiment. Also shown is the boiling temperature of the modeled metal system, calculated by regression through the calculated saturated pressure data. Again, the theory closely matches experiment.

As concluded in previous studies[1,2,3], the nearly free electron behavior of the metal system is an adequate representation of the liquid metal system, when modified to account for differences between the experimental and theoretical internal energy at the metal melting temperature. The hard-sphere fluid is an adequate liquid structure representation for both group IA and group IIA metals. Calculated thermodynamic properties of the metal systems are well within experimental error between the melting points and boiling points of the liquid metals.

The accuracy of the calculation is limited in two respects. The validity of the vapor phase model may be questioned at higher temperatures, as the density of the vapor

Table 1 Parameters used in the Gibbs-Bogoljubov calculation. Where parameters are not available for the diatomic vapor species the vapor is assumed to be an ideal monatomic gas. The experimental internal energies are based on those in J. M. Ziman[12]. Diatomic spectral data are from Huber and Herzberg[13]. Core radii are the values given by Hafner[14]. All other property data are taken from the *CRC Handbook of Chemistry and Physics*. 74th Edition[15].

	Molecular Weight	*Charge*	*Core Radius*	*Melting temperature Internal Energy*	*Melting Temperature*	*Boiling Temperature*	*Diatomic Ground State Energy*	*Diatomic Bond Length*	*Diatomic Vibrational Frequency*
		(a.u)	*(a.u)*	*(Hartrees)*	*(K)*	*(K)*	*(eV)*	$(10^{10} m)$	(cm^{-1})
Li	6.939	1.0	1.31	−0.1362	453.0	1615	1.046	2.673	351.43
Na	22.98	1.0	1.70	−0.1144	373.0	1156	0.720	3.079	159.124
K	39.10	1.0	2.12	−0.0954	336.4	1033	0.514	3.900	92.3
Rb	85.47	1.0	2.47	−0.0886	312.6	961	—	—	
Cs	132.91	1.0	2.72	−0.0836	301.6	944	0.394	4.47	42.022
Mg	24.31	2.0	1.31	−0.449	922	1363	0.0501	3.891	51.12
Ca	40.08	2.0	1.73	−0.368	1112	1757	0.12	4.2773	64.92

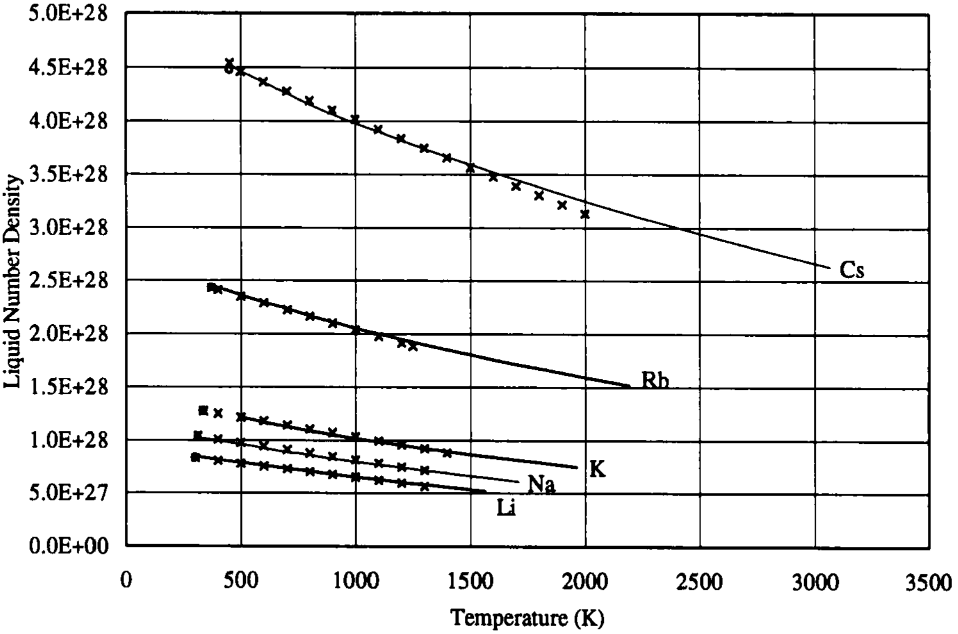

Figure 1 The continuous curves show calculated liquid number density (atoms/m^3) versus temperature for various Group IA metals. The assessed experimental data (x) are from Vargaftik[16]. The experimental melting temperature and density are marked by the circles.

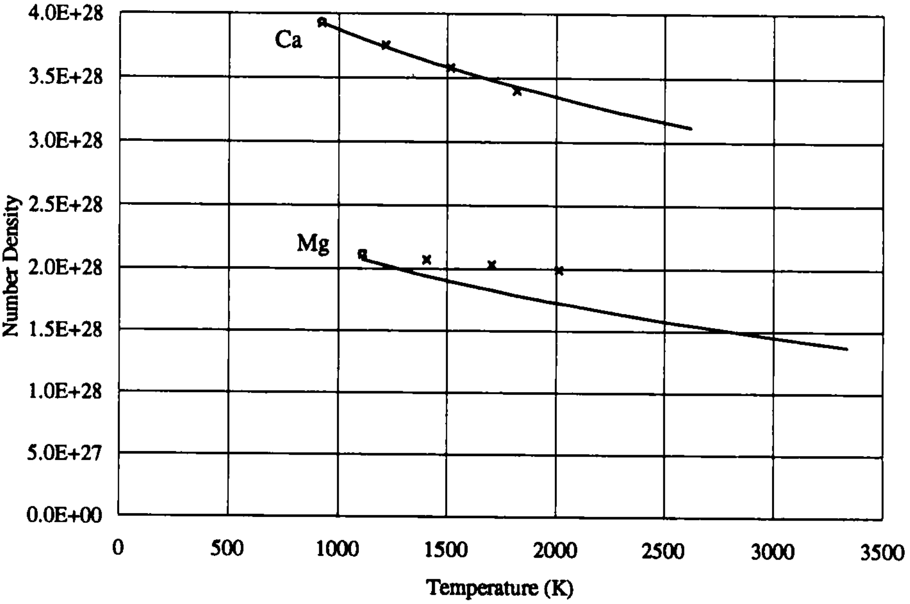

Figure 2 The continuous curves show the calculated number density (atoms/m^3) versus temperature (K) curve for select group IIA elements. The experimental data shown (x) are from the *CRC Handbook of Chemistry and Physics, 34th ed.*[15]. The experimental melting temperature and density are marked by the circles.

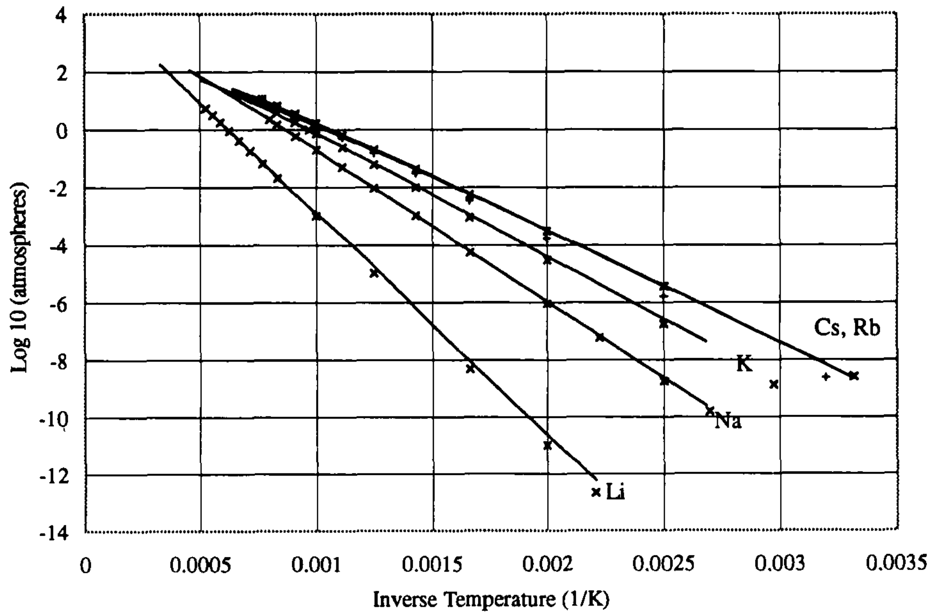

Figure 3 The $\log_{10}$(pressure in atmospheres) versus inverse temperature (1/K) curves for selected Group IA metals. The experimental points (x) are assessed data from Hultgren, *et al.*[17]. Rubidium assessed data is marked with the + symbol to distinguish the points from the data for cesium.

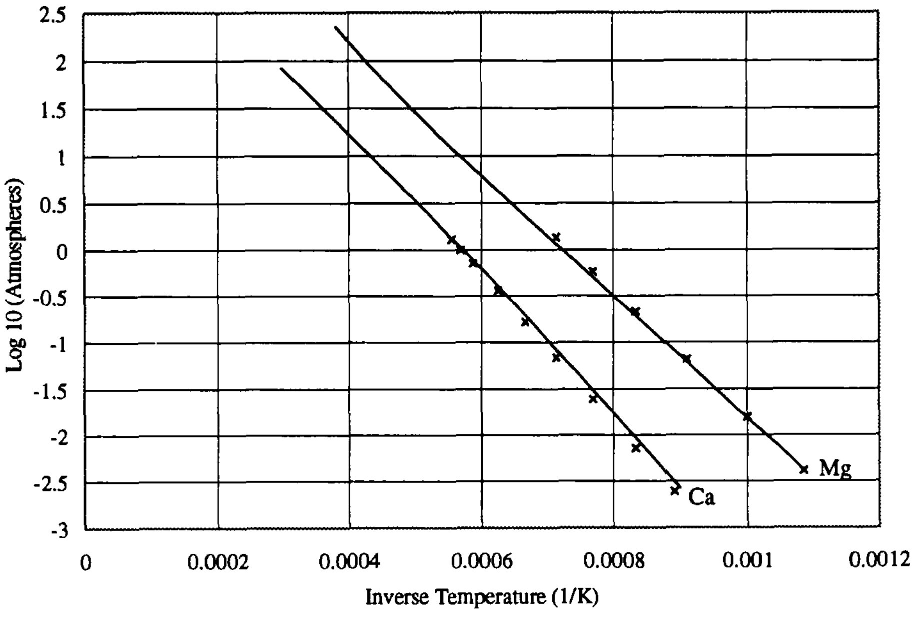

Figure 4 The $\log_{10}$(pressure in atmospheres) versus inverse temperature (1/K) curves for selected Group IIA metals. The experimental points (x) are assessed data from Hultgren, *et al.*[17].

Table 2 Ionization energy values, calculated to fit experimental data at the boiling temperature. Also included are the predicted melting temperatures from Antoine equation curve fits to the calculated pressure and temperature data ($\log_{10}(P) = A/T + B$). Experimental curves are from the *CRC Handbook of Chemistry and Physics*, 74th edition[15].

Element	*Experimental Ionization Energy (eV)*	*Calculated Ionization Energy (eV)*	*Experimental Boiling temperature (K)*	*Calculated Boiling temperature (K)*
Li	5.392	5.945	1615	1611
Na	5.139	5.235	1156	1163
K	4.341	4.410	1032	1053
Rb	4.177	4.095	961	980
Cs	3.894	3.824	944	952
Mg	22.681	23.22	1363	1380
Ca	17.984	18.62	1757	1768

phase increases. Just as the concentration of dimers increases with increasing temperatures and increasing density, so should the concentration of more complex clusters increase as the metal vapor reaches densities close to that of the liquid state.

The empty core representation of the potential energy function may also be an inaccurate representation of the metallic liquid at high temperatures, as the density of the liquid melt decreases. The metal-insulator transition in the alkali metals such as cesium occurs in the liquid arm of a density temperature plot[11]. For densities lower than the transition density the empty-core pseudopotential representation of the liquid metal is not valid, since the conduction electrons recombine in various arrangements with the metal ion cores. As a result, the postulated empty-core pseudopotential model is not capable of calculating the critical point of an alkali metal in its present form, since the model assumes an electron gas-ion core interaction at all liquid densities. A qualitatively different liquid phase potential which predicts the metal-insulator transition must be incorporated into the liquid model to match experimental results.

References

1. S. M. Osman and W. H. Young, *Chemistry of Liquids*, **17**, 181 (1987).
2. P. Minchin, M. Watabe, and W. H. Young, *Journal of Physics F: Metal Physics*, **7**, 563 (1977).
3. I. H. Umar, A. Meyer, M. Watabe, W. H. Young, *Journal of Physics F: Metal Physics*, **4**, 1691 (1974).
4. D. Pines, *The Theory of Quantum Liquids*, ed by D. F. Brewer, Benjamin, New York, New York, 1966.
5. L. Hedin and S. Lundqvist, *Solid State Physics*, ed. by F. Seitz and D. Turnbull, Academic Press, New York 1966.
6. S. Ichimaru and K. Utsumi, *Physical Review B* **24**, 7285 (1981).
7. N. W. Ashcroft and J. Lekner, *Physical Review*, **143**, 145 (1966).
8. N. W. Ashcroft, *Physics Letters* **23**, 48 (1966).
9. L. D. Landau and E. M. Lifshitz, *Statistical Physics, Part I*, Pergamon Press, New York, 1980.
10. D. McQuarrie, *Statistical Mechanics*, Harper & Row, New York, 1976.
11. R. G. Chapman and N. H. March, *Physical Review*, **B38**, 792 (1988).
12. J. M. Ziman, *The Physics of Metals-1. Electrons*, Cambridge University Press, New York, 1969.

13. K. P. Huber, G. Herzberg, *Molecular Spectra and Molecular Structure-IV. Constants of Diatomic Molecules*, Van Nostrand Reinhold Company, New York, 1952.
14. J. Hafner, *From Hamiltonians to Phase Diagrams, Springer Series in Solid State Sciences*, Springer, Berlin, 1987.
15. CRC *Handbook of Chemistry and Physics*, 74th Edition, CRC Press, Boca Raton, 1993.
16. N. B. Vargaftik, *Tables on the Thermophysical Properties of Liquids and Gases*, John Wiley and Sons, New York, 1975.
17. R. Hultgren, P. Desai, D. Hawkins, M. Gleiser, K. Kelley, and D. Wagman, *Selected Values of the Thermodynamic Properties of the Elements*, American Society for Metals, Metals Park, 1973.